A Dataset of Highly Accurate Homolytic N—Br Bond Dissociation Energies Obtained by Means of W2 Theory

Robert J. O'Reilly*[a] and Amir Karton[b]

Homolytic N—Br bond dissociation constitutes the initial step of numerous reactions involving N-brominated species. However, little is known about the strength of N—Br bonds toward homolytic cleavage. We herein report accurate bond dissociation energies (BDEs) for a set of 18 molecules using the high-level W2 thermochemical protocol. The BDEs (at 298 K) of the species in this set range from 162.2 kJ mol^{-1} (N-bromopyrrole) to 260.6 kJ mol^{-1} ((CHO)$_2$NBr). In order to compute BDEs of larger systems, for which W2 theory is not applicable, we have benchmarked a wide range of more economical theoretical procedures. Of these, G3-B3 offers the best performance (root-mean-square deviations = 2.9 kJ mol^{-1}), and using this method, we have computed N—Br BDEs for four widely used N-brominated compounds. These include (BDEs are given in parentheses): N-bromosuccinimide (281.6), N-bromoglutarimide (263.2), N-bromophthalimide (274.7), and 1,3-dibromo-5,5-dimethylhydantoin (218.2 and 264.8 kJ mol^{-1}). © 2015 Wiley Periodicals, Inc.

DOI: 10.1002/qua.25024

Introduction

The chemistry of N-brominated compounds (i.e., molecules containing an N—Br bond) is diverse, with such species being of significant importance in organic chemistry,[1–3] and biochemistry.[4–7] In addition, N-brominated biocidal polymers have also been developed for use in the disinfection of water[8-10] and sterilization of stainless steel surfaces.[11] Regarding the mechanisms by which N-brominated species react with organic molecules, while a number of reactions are known to proceed via ionic pathways (i.e., via the delivery of Br$^{\delta+}$),[12] many also proceed via free-radical mechanisms. In the case of many of the free-radical reactions, homolytic cleavage of an N—Br bond (affording a nitrogen-centered radical and bromine atom) constitutes the initiation step [Eq. (1)]:

$$RR'N–Br \rightarrow RR'N\bullet + Br\bullet \qquad (1)$$

Examples of reactions involving initial N—Br bond homolysis include: (i) The well-known Hofmann–Löffler–Freytag reaction, in which N-bromoalkylammonium derivatives containing a δ-hydrogen may be cyclized to form pyrrolidines,[13] (ii) The reaction between N-bromophthalimide and alkynes, in which the products are alkenes containing a bromine atom and imide moiety vicinal to each other,[14] (iii) The photochemical bromination reactions of alkanes affording bromoalkanes,[15] (vi) The degradation of extracellular matrix and its components via the formation of glycosaminoglycan-derived nitrogen-centered radicals,[5] and (v) The oxidation of alcohols to aldehydes or ketones with phenyl N-bromoketimine.[16]

Given that homolytic N—Br bond cleavage constitutes the initiation step for numerous reactions involving N-brominated species, knowledge of the strength of N—Br bonds is of the utmost importance. However, to the best of our knowledge, very little data exist in the literature concerning the strength of N—Br bonds toward homolysis. This article overcomes this void by: (i) computing highly accurate N—Br bond dissociation energies (BDEs) for 18 systems (which contain prototypical functional groups found in synthetically-relevant N-brominated species) using the W2 thermochemical protocol,[17] (ii) assessing the performance of a wide range of more economical theoretical procedures (namely, density functional theory (DFT), double hybrid DFT (DHDFT), standard and composite ab initio methods) for their ability to accurately calculate N—Br BDEs, and (iii) using the best performing lower-cost theoretical method to compute N—Br BDEs for four widely employed N-brominated species (namely the N-bromo derivatives of succinimide, glutarimide, phthalimide, and the dibrominated derivative of 5,5-dimethylhydantoin).

Computational Details

The geometries of all species were obtained at the B3LYP/A'VTZ level (where A'VnZ indicates the combination of cc-pVnZ for H and aug-cc-pVnZ for all other elements),[18,19] and were confirmed to be equilibrium structures (i.e., consisting of all real frequencies) by way of harmonic vibrational frequency calculations, which were performed at the same level of theory. The zero-point vibrational energy (ZPVE) and enthalpy (H_{vib}(298 K)) corrections resulting from these frequency calculations have been used in later steps (vide infra). These corrections have been scaled according to literature scaling factors, namely 0.9884 for the ZPVE and 0.9987 for H_{vib}(298 K).[20] All

[a] R. J. O'Reilly
    Department of Chemistry, School of Science and Technology, Nazarbayev University, Astana, Republic of Kazakhstan
    E-mail: robert.o'reilly@nu.edu.kz
[b] A. Karton
    School of Chemistry and Biochemistry, the University of Western Australia, Perth, Western Australia, 6009, Australia

geometry optimizations and frequency calculations were performed using Gaussian 09 (Revision D.01).[21]

High-level N—Br BDEs were then obtained at the W2 level[17] (using the Molpro 2012.1 program suite),[22] as described in Ref. 23. For the sake of keeping this article self-contained, the steps involved in obtaining the W2 energies are briefly described. The ROHF component is obtained by way of a two-point extrapolation (using the $E(L) = E_\infty + A/L^5$ formula) based on energies obtained in conjunction with the A′VQZ and A′V5Z basis sets. The valence ROCCSD correlation energy is obtained using the same basis sets, but with the $E(L) = E_\infty + A/L^3$ two-point extrapolation formula. The (T) valence correlation component is obtained with the same extrapolation formula, but in conjunction with the A′VTZ and A′VQZ basis sets. The inner-shell correlation contribution is obtained at the CCSD(T) level using the MTsmall basis set.[17] For bromine atom and bromine-containing molecules, the five lowest energy orbitals of bromine (i.e., 1s, 2s and 2p) orbitals are frozen. The scalar-relativistic contribution is obtained from second-order Douglass–Kroll–Hess[24,25] CCSD(T)/MTsmall calculations. An atomic spin-orbit correction of 14.69 kJ mol^{-1} has been applied to Br•.[26] In addition, scaled ZPVE and H_{vib}(298 K) corrections have been included, leading to BDEs at 298 K (vide supra).

The DFT exchange-correlation functionals considered in this study (ordered by their rung on Jacob's Ladder)[27] are the pure generalized gradient approximation (GGA) functionals: BLYP,[28,29] B97-D,[30] HCTH407,[31] PBE,[32] BP86,[29,33] SOGGA11,[34] and N12;[35] the meta-GGAs (MGGAs): M06-L,[36] TPSS,[37] τ-HCTH,[38] VSXC,[39] M11-L,[40] and MN12-L;[41] the hybrid-GGAs (HGGAs): BH&HLYP,[42] B3LYP,[28,43,44] B3P86,[33,44] B3PW91,[44,45] PBE0,[46] B97-1,[47] B98,[48] X3LYP,[49] and SOGGA-11X;[50] the hybrid-meta-GGAs (HMGGAs): M05,[51] M05-2X,[52] M06,[53] M06-2X,[53] M06-HF,[53] BMK,[54] B1B95,[29,55] PW6B95,[56] TPSSh,[57] and τ-HCTHh;[38] the DHDFT procedures (which have been evaluated within the frozen-core approximation):[58] B2-PLYP,[59] ROB2-PLYP,[60] B2GP-PLYP,[61] B2K-PLYP,[62] B2T-PLYP,[62] DSD-BLYP,[63] DSD-PBEP86,[64,65] and PWPB95.[66] In addition to the global HGGAs and HMGGAs, we also consider the following range-separated (RS) functionals: CAM-B3LYP,[67] LC-ωPBE,[68] ωB97,[69] ωB97X,[69] ωB97X-D,[70] HSE06,[71] HISS,[72] N12-SX,[73] MN12-SX[73] and M11.[74] For some functionals, we have also included empirical D3 dispersion corrections,[75–77] which make use of the Becke–Johnson[78] damping potential as recommended in Ref. 75 (denoted by the suffix-D3). The standard DFT calculations were carried out in conjunction with the A′VTZ basis set, while the DHDFT calculations, due to their slower basis set convergence,[79] were carried out with the A′VQZ basis set.

In addition, the performance of various composite thermochemical procedures and standard ab initio methods are also assessed. We consider the following composite procedures (which we have run using the respective keywords in Gaussian 09): G4,[80] G4(MP2),[81] G4(MP2)−6X,[82] G3-B3,[83] G3(MP2)-B3,[83] CBS-QB3,[84] and ROCBS-QB3.[85] It should be noted that the G3-B3 calculations reported in section 3.6 are based on the use of geometries (and harmonic vibrational frequencies) obtained at the B3LYP level in conjunction with the larger

Table 1. Component breakdown and final homolytic N—Br bond dissociation energies at 298 K (kJ mol^{-1}).

Molecule	ΔSCF	ΔCCSD	Δ(T)	ΔCV	ΔRel.	BDE$_e$[a]	BDE$_{298}$[b]
NH$_2$Br (1)	100.2	125.9	18.2	2.1	−2.4	246.4	217.4
NH$_3$Br$^+$ (2)	134.6	128.5	16.0	1.3	0.0	280.5	252.4
MeNHBr (3)	86.9	124.9	19.3	2.1	−2.1	233.1	206.5
MeNH$_2$Br$^+$ (4)	99.6	117.1	15.9	1.0	0.0	233.6	205.2
Me$_2$NBr (5)	70.0	127.2	20.7	2.1	−1.8	219.9	195.4
Me$_2$NHBr$^+$ (6)	63.8	121.1	17.9	1.0	0.0	203.8	177.6
CF$_3$NHBr (7)	87.1	130.0	18.9	2.4	−2.1	238.4	214.2
N-BrImidazole (8)	64.0	104.4	17.0	3.7	−2.6	189.0	165.4
N-BrPyrrole (9)	64.1	102.2	16.4	3.7	−2.7	186.5	162.2
HCONHBr (10)	134.8	108.3	15.6	2.8	−2.9	261.4	236.2
MeCONHBr (11)	123.8	114.0	15.7	2.6	−2.8	256.1	230.7
FCONHBr (12)	116.8	119.0	15.5	2.7	−2.7	254.0	228.7
(NC)CONHBr (13)	134.2	112.3	15.8	2.8	−2.7	265.2	239.7
HCONMeBr (14)	113.7	115.5	18.3	2.6	−2.7	250.1	225.0
H$_2$NCONHBr (15)	103.2	122.2	17.9	2.5	−2.5	245.8	221.1
(CHO)$_2$NBr (16)	143.1	122.0	17.7	2.6	−2.2	285.4	260.6
H$_2$C=NBr (17)	55.5	122.7	20.7	1.7	−1.5	200.6	176.5
MeCH=NBr (18)	59.9	124.5	21.2	1.8	−1.6	207.3	185.4

[a] All-electron, vibrationless, nonrelativistic N—Br bond energies which are used for assessing DFT, DHDFT, and composite and standard ab initio procedures. [b] N—Br bond dissociation energies at 298 K, which include scalar relativistic effects, a spin-orbit contribution for Br•, and zero-point vibrational energy, and enthalpy corrections (the ZPVE and H_{vib}(298 K) corrections are given in Supporting Information Table S2).

A′VTZ, rather than the default 6-31G(d), basis set. We consider the following ab initio methods: MP2, SCS-MP2,[86] MP3, MP3.5,[87] SCS-MP3,[88] MP4, MP4$_{avr}$,[89] CCSD, and CCSD(T). All DFT, DHDFT, composite thermochemical and standard ab initio calculations were performed using Gaussian 09 (Revision D.01)[21] and ORCA (Version 3.0.1).[90,91] To assist in the analysis of substituent effects, natural bond orbital (NBO) calculations[92] at the B3LYP/A′VTZ level have been performed using Gaussian 09 (Revision D.01).

Results and Discussion

Overview of the set of 18 N–Br BDEs

We begin by briefly introducing the set of 18 homolytic N—Br bond dissociation energies (BDEs), which we have obtained using the high-level W2 thermochemical protocol (Table 1). We have tabulated both electronic values (BDE$_e$) and values corrected to 298 K (BDE$_{298}$). Since W2 theory constitutes a layered extrapolation to the CCSD(T) basis-set-limit, it is of interest to estimate whether post-CCSD(T) excitations are likely to contribute significantly to the bottom-of-the-well, nonrelativistic electronic BDEs. The percentage of the total atomization energy accounted for by parenthetical connected triple excitations, %TAE$_e$[(T)], has been shown to be a reliable energy-based indicator as to the importance of post-CCSD(T) contributions.[93–95] It has been suggested that %TAE$_e$[(T)] < 2 indicates systems that are dominated by dynamical correction, while 2 < %TAE$_e$[(T)] < 5 indicates systems that include mild nondynamical correlation.[93] The %TAE$_e$[(T)] values for all

Figure 1. Mulliken spin densities for the pyrrolyl and imidazolyl radicals obtained at the B3LYP/A'VTZ level.

of the species involved in obtaining the N—Br BDEs range from 0.6 ($NH_3^{\bullet+}$) to 3.9% ((NC)CONHBr) (Supporting Information Table S1). These values indicate the reliability of the CCSD(T) method for the calculation of bottom-of-the-well BDEs, and indicate that such values should be well within ~1 kcal mol^{-1} from the full configuration interaction (FCI) basis-set limit.

From a theoretical perspective, it is of interest to briefly consider the contributions of the various components to the BDEs (Table 1). As is to be expected, the underlying Hartree–Fock (i.e., ΔSCF) components represent drastic underestimations of the BDEs. In that regard, the inclusion of the ΔCCSD contribution serves to substantially increase the BDEs. Inclusion of parenthetical triples excitations (i.e., Δ(T)) further increase the energies, although by much smaller amounts compared with the ΔCCSD corrections. The core-valence correlation terms (i.e., ΔCV) adopt positive values ranging from 1.0 to 3.7 kJ mol^{-1}, and for the most part, are almost cancelled by the relativistic corrections (ΔRel.) (i.e., the sum of these components ranges from −0.3 to +0.4 kJ mol^{-1}). The main exception to this is for the N-bromoammonium species, where the relativistic corrections are negligible.

The parent system, NH$_2$Br, is computed to have a BDE$_{298}$ value of 217.4 kJ mol^{-1}, but upon the introduction of substituents, the BDE$_{298}$ values range from 162.2 kJ mol^{-1} (N-bromopyrrole) to 260.6 kJ mol^{-1} ((CHO)$_2$NBr). The comparatively low BDEs of the heterocyclic systems N-bromopyrrole (162.2 kJ mol^{-1}) and N-bromoimidazole (165.4 kJ mol^{-1}), may be attributed, in part, to the relative stabilization of the radical products. In particular, in contrast to the radicals arising via the dissociation of the other 16 species, the unpaired electrons in the pyrrolyl and imidazolyl radicals are delocalized on the less electronegative carbon atoms rather than on nitrogen, as demonstrated by Mulliken spin densities (obtained at the B3LYP/A'VTZ level, Fig. 1).

By way of contrast, introduction of two electron-withdrawing formyl substituents to the nitrogen center (as in (CHO)$_2$NBr) results in the largest N—Br BDE (260.6 kJ mol^{-1}). This finding can be rationalized using the same arguments invoked previously in accounting for the relatively large N—H BDEs of imides.[96–98] In particular, strong stabilizing interactions between the lone-pair of nitrogen and the $\pi^*_{C=O}$ orbitals of the carbonyl groups in (CHO)$_2$NBr are largely lost upon formation of (CHO)$_2$N•. This is consistent with our finding, and the findings of others,[97,99] that (CHO)$_2$N• adopts a π- rather than σ-ground state. Thus, in the radical, it is the unpaired electron, not the lone pair, that interacts with the carbonyl substituents.

To quantify the magnitude of delocalization effects that are lost upon going from the closed-shell parent ((CHO)$_2$NBr) to the radical product ((CHO)$_2$N•), we have performed NBO calculations at the B3LYP/A'VTZ level. In particular, we find that whereas the two lone-pair → $\pi^*_{C=O}$ interactions in (CHO)$_2$NBr are associated with especially large stabilization energies ($E_{(2)}$) of 188.0 kJ mol^{-1} per interaction, the two largest such interactions in (CHO)$_2$N• have $E_{(2)}$ values of just 19.2 and 21.5 kJ mol^{-1}. The same effects, although smaller in magnitude, also account for the relatively large BDEs of the monocarbonyl-containing species, which range from 221.1 (H$_2$NCONHBr) to 239.7 ((NC)CONHBr) kJ mol^{-1}. Previous theoretical[97–100] and experimental studies[101–104] support the notion that amidyl radicals, of the type considered in this investigation, adopt a π- rather than σ-ground state.

The commercially available reagent N-bromoacetamide (CH$_3$CONHBr), which may be prepared via the reaction of acetamide with bromine under strongly alkaline conditions,[105] is computed to have a BDE of 230.7 kJ mol^{-1}. The larger BDE of N-bromoacetamide compared with the BDEs of MeNHBr (206.5) and Me$_2$NBr (195.4 kJ mol^{-1}), is consistent with experimental observations indicating that the former possesses greater stability. In this regard, although CH$_3$CONHBr is a solid with a melting point of 102–105°C,[105] MeNHBr and Me$_2$NBr are relatively shorter-lived species.[106,107] The N-bromo derivative of urea (H$_2$NCONHBr), which has been used in the selective oxidation of tryptophan residues[108,109] is associated with a slightly smaller BDE (221.1 kJ mol^{-1}) when compared with CH$_3$CONHBr.

In comparison with the BDEs of MeNHBr (206.5) and Me$_2$NBr (195.4 kJ mol^{-1}), the conjugate acids of these species (i.e., MeNH$_2$Br$^+$ and Me$_2$NHBr$^+$) are associated with BDEs that are reduced by 1.3 and 17.8 kJ mol^{-1}, respectively. This finding supports the notion that the strongly acidic conditions employed in the Hoffman–Löffler–Freytag reaction facilitate thermally induced homolytic N—Br cleavage.[13] Also of note are the relatively low BDEs of the N-bromoimine derivatives, H$_2$C=NBr and MeCH=NBr, for which we compute values of 176.5 and 185.4 kJ mol^{-1}, respectively. The relatively low BDEs of such species support the proposal that N-bromoketimine-induced oxidation of alcohols to aldehydes or ketones proceeds via a mechanism involving the formation of an iminyl radical.[16]

Finally, it is of interest to point out that although N-chloropyrrole has been isolated and studied,[110] N-bromopyrrole remains elusive. It seems plausible that the particularly low N—Br BDE of N-bromopyrrole (162.2 kJ mol^{-1}) would render the production of this compound a significant challenge, especially given that the N—Cl bond of N-chloropyrrole is substantially stronger (203.7 kJ mol^{-1}).[111] However, it should be noted that even 2- and 3-bromopyrrole, species that contain stronger C—Br bonds, are also known to possess very limited stability.[112]

Performance of conventional DFT procedures for the calculation of N—Br BDEs

We have assessed the performance of 53 conventional DFT procedures across the set of 18 N—Br BDEs provided in Table

1. It is important to point out that we are comparing the DFT values with W2 energies (BDE$_e$) that do not include secondary effects not explicitly accounted for in the DFT procedures (i.e., relativistic, ZPVE, and spin-orbit effects). Table 2 gives the root-mean-square deviations (RMSDs), mean absolute deviations (MADs), mean signed deviations (MSDs), and number of outliers (NOs, arbitrarily defined as the number of species having deviations ≥ 10 kJ mol^{-1}), from the benchmark W2 results. Regarding the performance of the considered procedures, we make the following general observations:

Of the 53 functionals that we have considered (i.e., GGA, MGGA, HGGA, HMGGA, and RS), none attain RMSDs below the threshold of chemical accuracy (≤ 4.2 kJ mol^{-1}). In particular, $\sim 90\%$ of the functionals have RMSDs that are >10 kJ mol^{-1}.

The inclusion of the D3-dispersion correction offers moderate to large improvements in performance (by amounts ranging from 0.5 (BP86) to 13.5 (BLYP) kJ mol^{-1}), except in the case of PBE (where a deterioration of 1.9 kJ mol^{-1} is seen).

The best performing methods are: BMK-D3 (RMSD = 7.0), MN12-SX (7.4), M11 (7.4), and M06-HF (7.8 kJ mol^{-1}). In contrast, BH&HLYP offers by far the worst performance (RMSD = 55.4 kJ mol^{-1}), although other poor performing methods include: M05 (34.2), B3LYP (31.1), and HCTH407 (30.1 kJ mol^{-1}).

For 44 of the 53 functionals surveyed, the largest deviations were associated with molecule **6** (Me$_2$NHBr$^+$).

An overwhelming majority of the functionals underestimate the BDEs, with most doing so systematically (i.e., MSD = $-1\times$ MAD). Only six of the considered functionals are associated with positive MSDs, and with the exception of M06-HF, they all belong to the GGA family.

Beginning with the performance of the GGAs, for which we have evaluated 10 such functionals, the best performing methods exhibit RMSDs of 11.0 (PBE) and 11.4 (BP86-D3) kJ mol^{-1}. In contrast, the worst performing procedures are: HCTH407 (30.1), BLYP (29.4), and SOGGA11 (29.1 kJ mol^{-1}). As for the effect of including the D3 dispersion correction, we find that: (i) the RMSD of BLYP-D3 (15.9 kJ mol^{-1}) is 13.5 kJ mol^{-1} lower than the parent BLYP functional, (ii) only a very modest improvement (of 0.5 kJ mol^{-1}) is noted in the case of BP86 vs. BP86-D3, and (iii) of all of the conventional DFTs surveyed, PBE is the only functional for which inclusion of the D3 term results in a deterioration in performance (by 1.9 kJ mol^{-1}).

Moving up one rung of Jacob's ladder to the MGGAs (which include the kinetic energy density), we do not find any substantive improvement in performance compared with the GGAs. The best performing methods of this class are M11-L and TPSS-D3 (with RMSDs of 10.5 and 10.9 kJ mol^{-1}, respectively), while the worst performing methods are τ-HCTH (24.3) and VSXC (28.9 kJ mol^{-1}). All of the considered MGGAs tended to underestimate the bond energies. The inclusion of a D3 correction was only investigated in the case of TPSS, and doing so resulted in a substantial improvement in performance (by 7.2 kJ mol^{-1}).

The HGGA procedures offer performance that is comparable to that of the GGAs and MGGAs. Namely, the best performing

Table 2. Statistical performance of conventional DFT procedures for the calculation of homolytic N—Br bond dissociation energies relative to W2 reference values (kJ mol^{-1}).[a,b]

Type[c]	Method	RMSD	MAD	MSD	LD	NO
GGA	HCTH407	30.1	27.9	−27.9	53.0 (**6**)	17
	BLYP	29.4	27.1	−27.1	44.6 (**6**)	17
	SOGGA11	29.1	26.4	+26.0	45.2 (**2**)	16
	B97-D3	20.6	18.8	−18.8	32.2 (**16**)	13
	BLYP-D3	15.9	13.6	−12.6	27.0 (**16**)	12
	N12	13.9	12.0	+8.8	26.3 (**8**)	9
	PBE-D3	12.9	10.3	+8.1	24.0 (**8**)	7
	BP86	11.9	10.4	−4.9	26.2 (**6**)	8
	BP86-D3	11.4	9.2	+6.7	22.4 (**8**)	6
	PBE	11.0	9.1	+1.8	20.7 (**6**)	8
MGGA	VSXC	28.9	28.3	−28.3	41.2 (**4**)	18
	τ-HCTH	24.3	22.0	−22.0	45.2 (**6**)	15
	MN12-L	22.7	22.0	−22.0	36.9 (**6**)	18
	M06-L	20.3	18.6	−18.6	38.2 (**6**)	16
	TPSS	18.1	15.6	−15.6	32.5 (**6**)	12
	TPSS-D3	10.9	9.4	−7.2	20.0 (**6**)	7
	M11-L	10.5	9.0	−7.9	23.1 (**6**)	7
HGGA	BH&HLYP	55.4	55.3	−55.3	64.9 (**6**)	18
	B3LYP	31.1	30.3	−30.3	45.8 (**6**)	18
	X3LYP	29.1	28.4	−28.4	43.6 (**6**)	18
	B3PW91	22.2	21.0	−21.0	40.4 (**6**)	18
	SOGGA11-X	21.5	20.9	−20.9	32.6 (**6**)	17
	B98	20.5	19.3	−19.3	35.5 (**6**)	16
	B3LYP-D3	19.1	18.4	−18.4	28.3 (**6**)	16
	PBE0	16.4	15.0	−15.0	33.6 (**6**)	13
	B97-1	16.1	14.5	−14.5	30.6 (**6**)	13
	B3P86	11.9	9.7	−9.6	28.8 (**6**)	9
	PBE0-D3	10.9	9.2	−9.2	25.1 (**6**)	7
	B3PW91-D3	10.5	9.0	−8.8	22.5 (**6**)	8
HMGGA	M05	34.2	33.4	−33.4	50.2 (**6**)	18
	TPSSh	22.4	21.2	−21.2	37.3 (**6**)	17
	BMK	15.5	14.4	−14.4	29.8 (**6**)	13
	PW6B95	15.2	13.8	−13.8	30.7 (**6**)	14
	τ-HCTHh	14.8	12.8	−12.7	30.7 (**6**)	11
	B1B95	14.3	12.4	−12.4	32.0 (**6**)	12
	M06-2X	14.2	13.8	−13.8	20.2 (**6**)	17
	M06	12.8	11.6	−11.6	23.2 (**6**)	12
	M05-2X	12.2	11.8	−11.8	17.0 (**6**)	12
	PW6B95-D3	11.5	10.0	−9.9	25.2 (**6**)	7
	M06-HF	7.8	6.8	+6.5	14.5 (**5**)	3
	BMK-D3	7.0	5.4	−4.5	16.0 (**6**)	3
RS	CAM-B3LYP	27.6	27.0	−27.0	40.7 (**6**)	18
	LC-ωPBE	26.6	25.8	−25.8	39.6 (**6**)	18
	HISS	25.2	24.3	−24.3	40.3 (**6**)	18
	CAM-B3LYP-D3	21.8	21.2	−21.2	32.4 (**6**)	18
	ωB97	20.3	19.7	−19.7	30.0 (**5**)	17
	LC-ωPBE-D3	20.1	19.0	−19.0	29.9 (**5,6**)	18
	ωB97X	19.7	19.0	−19.0	29.4 (**6**)	17
	ωB97X-D	18.7	17.9	−17.9	31.0 (**6**)	17
	HSE06	17.1	15.8	−15.8	34.0 (**6**)	15
	N12-SX	9.5	6.7	−5.2	27.4 (**6**)	3
	MN12-SX	7.4	5.6	−5.6	19.2 (**6**)	4
	M11	7.4	5.6	−4.6	15.9 (**6**)	4

[a] The calculations are carried out in conjunction with the A'VTZ basis set. [b] RMSD = root mean square deviation, MAD = mean absolute deviation, MSD = mean signed deviation, LD = largest deviation in absolute value (the molecule associated with the largest deviation is indicated in parentheses), NO = number of outliers (species with deviations from W2 reference values ≥ 10 kJ mol^{-1}). [c] GGA = generalized gradient approximation, HGGA = hybrid-GGA, MGGA = meta-GGA, RS = range-separated, HMGGA = hybrid meta-GGA.

Table 3. Statistical performance of DHDFT procedures for the calculation of homolytic N—Br bond dissociation energies relative to W2 reference values (kJ mol^{-1}).[a,b]

Method	RMSD	MAD	MSD	LD	NO
DSD-PBEP86-D3	11.6	9.3	+9.3	22.9 (**13**)	7
B2-PLYP	10.6	9.6	−9.6	19.4 (**6**)	9
B2T-PLYP	10.3	9.1	−9.1	18.1 (**6**)	7
DSD-PBEP86	8.3	6.6	+4.8	18.5 (**13**)	4
B2GP-PLYP	7.7	6.6	−5.5	14.0 (**6**)	5
B2K-PLYP	7.1	6.3	−2.7	10.6 (**6**)	2
DSD-BLYP	7.0	5.8	+2.7	15.5 (**13**)	3
B2K-PLYP-D3	6.8	6.0	0.0	12.8 (**13**)	1
PWPB95	6.6	5.3	−5.1	15.6 (**6**)	2
ROB2-PLYP	6.2	5.0	−4.7	12.9 (**6**)	2
B2-PLYP-D3	5.7	5.0	−3.7	10.8 (**6**)	1
B2GP-PLYP-D3	5.7	5.1	−0.2	9.3 (**13**)	0
PWPB95-D3	4.3	3.4	−1.7	11.0 (**6**)	1

[a] These calculations were performed in conjunction with the A'VQZ basis set. [b] Abbreviations are defined in Footnote b of Table 2.

Table 4. Statistical performance of composite thermochemical protocols for the calculation of homolytic N—Br bond dissociation energies relative to W2 reference values (kJ mol^{-1}).[a]

Method	RMSD	MAD	MSD	LD	NO
CBS-QB3	9.8	8.1	+8.1	16.4 (**2**)	7
G4(MP2)	6.7	5.8	−5.8	13.5 (**16**)	3
G4(MP2)−6X	5.7	5.0	−5.0	11.8 (**16**)	1
ROCBS-QB3	4.5	3.7	+0.8	8.1 (**2**)	0
G4	4.3	3.7	−3.6	7.9 (**16**)	0
G3(MP2)-B3	4.2	3.6	−3.6	7.3 (**16**)	0
G3-B3	2.9	2.4	−2.1	5.2 (**1**)	0

[a] Abbreviations are defined in Footnote b of Table 2.

methods are B3PW91-D3 (RMSD = 10.5), PBE0-D3 (10.9), and B3P86 (11.9 kJ mol^{-1}). Of all the conventional DFTs investigated, the HGGA procedure BH&HLYP offered by far the worst performance (RMSD = 55.4 kJ mol^{-1}). The popular B3LYP functional performs quite poorly with an RMSD of 31.1 kJ mol^{-1} and an LD of 45.8 kJ mol^{-1}. As for the effect of the D3 dispersion correction, performance improvements of 5.5, 11.7 and 12.0 kJ mol^{-1} were noted in the case of PBE0, B3PW91, and B3LYP, respectively.

Of the HMGGA procedures, the best performance is noted in the case of BMK-D3 (RMSD = 7.0) and M06-HF (7.8 kJ mol^{-1}). For both of these procedures, the number of outliers is just three, with largest deviations of 16.0 and 14.5 kJ mol^{-1}, respectively. The worst performing method is M05, with an RMSD of 34.2 and an LD of 50.2 kJ mol^{-1}. Although all of the HMGGAs tend to systematically underestimate the BDEs (with the MSDs ranging from −4.5 to −33.4 kJ mol^{-1}), M06-HF systematically overestimates them (MSD = +6.5 kJ mol^{-1}).

Moving now to the range-separated functionals, we find that only three of the 12 procedures are associated with RMSDs below 10 kJ mol^{-1}, namely: M11 (7.4), MN12-SX (7.4), and N12-SX (9.5 kJ mol^{-1}). In fact, the next best method of this class is HSE06, with an RMSD of 17.1 kJ mol^{-1}. The worst performing methods are HISS, LC-ωPBE, and CAM-B3LYP with RMSDs of 25.2, 26.6, and 27.6 kJ mol^{-1}, respectively.

Performance of DHDFT procedures for the calculation of N—Br BDEs

Attention is now turned to the performance of various DHDFT procedures, which extend upon conventional DFTs by additionally including the virtual orbitals. Due to the slower basis set convergence of DHDFTs vs conventional DFT methods, we have used the larger A'VQZ basis set, rather than A'VTZ, for evaluating these methods. The statistical performance of these methods is provided in Table 3.

Of the 13 DHDFT procedures considered, 10 are associated with RMSDs that are lower than 10 kJ mol^{-1}, though none

offer RMSDs below the threshold of chemical accuracy ($\leq$4.2 kJ mol^{-1}). The best performing method is PWPB95-D3 (RMSD = 4.3 kJ mol^{-1}), while the next best performing methods are B2-PLYP-D3 and B2GP-PLYP-D3, both exhibiting RMSDs of 5.7 kJ mol^{-1}. With regards to the two latter procedures, although they have the same RMSDs, B2GP-PLYP-D3 offers a slightly lower LD (9.3 vs. 10.8 kJ mol^{-1}). We find that the inclusion of the D3 dispersion correction leads to improved results (by amounts ranging from 0.3 (B2K-PLYP) to 4.9 (B2-PLYP) kJ mol^{-1}), except in the case of DSD-PBEP86, where a deterioration of 3.3 kJ mol^{-1} is seen. As many of the considered radicals exhibit relatively large spin contamination, it is insightful to note that ROB2-PLYP, which makes use of a restricted-open shell wave function, offers significantly better performance (by 4.4 kJ mol^{-1}) compared with B2-PLYP, which uses an unrestricted wave function. We have additionally performed calculations in conjunction with the smaller A'VTZ basis set for the majority of the functionals in Table 3. For the considered functionals, we note that the use of the A'VTZ basis set offers RMSDs that are generally larger by amounts ranging from 0.8 (B2K-PLYP-D3) to 2.9 (B2T-PLYP) kJ mol^{-1} (Supporting Information Table S6).

Performance of composite thermochemical protocols for the calculation of N–Br BDEs

Attention is now given to the performance of a number of composite thermochemical protocols. We have considered the following Gaussian-n procedures: G3-B3, G3(MP2)-B3, G4, G4(MP2), and G4(MP2)−6X. In addition, we have considered the Complete Basis Set (CBS) methods: CBS-QB3 and ROCBS-QB3. When assessed against the highly accurate atomization energies of 124 nonmultireference systems contained in the W4-11 dataset,[95] these methods attained RMSDs of between 7.5–8.4 kJ mol^{-1}, with the exception of G4(MP2)−6X which offered substantially better performance (RMSD = 4.6 kJ mol^{-1}). The statistical performance of these methods for the calculation of N–Br BDEs is provided in Table 4.

We find that G3-B3 offers exceptional performance, with an RMSD and LD of just 2.9 and 5.2 kJ mol^{-1}, respectively. The computationally more efficient G3(MP2)-B3 procedure exhibits slightly worse performance (RMSD = 4.2 kJ mol^{-1}), but which is comparable to that of the significantly more costly G4 protocol (4.3 kJ mol^{-1}). The reduced-order variant of G4, namely

Table 5. Statistical performance of standard *ab initio* levels for the calculation of homolytic N—Br bond dissociation energies relative to W2 reference values (kJ mol^{-1})[a]

| Method[b]	RMSD	MAD	MSD	LD	NO
UMP2	60.7	55.4	+55.4	117.7 (**13**)	18
ROMP2	34.1	33.2	+33.2	46.0 (**16**)	18
UMP4(SDTQ)	33.8	29.6	+29.6	71.0 (**13**)	16
SCS-ROMP2	33.7	33.2	+33.2	41.6 (**6**)	18
URCCSD	23.2	23.1	−23.1	26.6 (**18**)	18
SCS-ROMP3	23.0	22.4	+22.4	31.2 (**6**)	18
ROMP4(SDTQ)	17.2	16.5	+16.5	25.3 (**16**)	16
ROMP3	10.7	9.8	−9.8	17.2 (**1**)	8
UMP3	10.6	8.7	−0.4	29.0 (**13**)	6
UMP4(SDQ)	10.3	8.3	−2.6	24.9 (**13**)	6
ROMP4(SDQ)	10.0	9.1	−9.1	16.6 (**1**)	7
URCCSD(T)	6.0	5.9	−5.9	7.1 (**1**)	0
ROMP4$_{av}$	5.7	4.8	+3.7	10.4 (**16**)	1
ROMP3.5	5.4	4.6	+3.4	9.0 (**16**)	0

[a] Abbreviations are defined in Footnote b of Table 2. [b] The single-level *ab initio* calculations were carried out in conjunction with the A'VQZ basis set.

G4(MP2), offers the second worst RMSD (6.7 kJ mol^{-1}) of all of the considered methods, though the closely related G4(MP2)−6X procedure offers a slight improvement (5.7 kJ mol^{-1}). The relatively poor performance of G4(MP2) has also been observed for the calculation of N—H and N—Cl BDEs.[113] The CBS-QB3 procedure is the worst performing of all the considered thermochemical protocols (RMSD = 9.8 kJ mol^{-1}). However, the related ROCBS-QB3 procedure, which makes use of the restricted-open-shell formalism for radical species offers a marked improvement (RMSD = 4.5 kJ mol^{-1}). In addition, we note that with the exception of CBS-QB3 and ROCBS-QB3, the Gaussian-n protocols systematically underestimate the BDEs (i.e., the MSDs are negative).

Performance of standard *ab initio* methods for the calculation of N—Br BDEs

We now turn our attention to the performance of a number of stand-alone *ab initio* methods, which are evaluated in conjunction with the A'VQZ basis set, and using the frozen-core approximation (Table 5). As the product radicals exhibit low to relatively high degrees of spin contamination (i.e., the $\langle s^2 \rangle$ values range from 0.76 to 1.08 (Supporting Information Table S1), where 0.75 indicates a pure doublet), we have considered the performance of some of the methods using both the unrestricted and restricted-open-shell formalisms (i.e., UMPn vs. ROMPn). The results of these methods are provided in Table 5.

To begin, we note that a substantial improvement in performance is observed on going from (RMSDs are given in parentheses): (i) UMP2 (60.7) → UMP3 (10.6 kJ mol^{-1}), and (ii) ROMP2 (34.1) → ROMP3 (10.7 kJ mol^{-1}). Moving to the performance of the MP4 methods, although UMP4(SDQ) and ROMP4(SDQ) offer modest improvements compared with their unrestricted/restricted MP3 counterparts (by 0.3 and 0.7 kJ mol^{-1}, respectively), the additional inclusion of triples, as in UMP4(SDTQ) and ROMP4(SDTQ), appears to be detrimental (RMSDs = 33.8 and 17.2 kJ mol^{-1}, respectively).
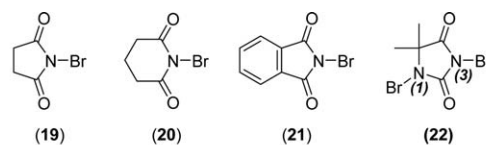
N-Br BDEs: 281.6   263.2   274.7   N(1) 218.2
(*kJ mol^{-1}, 298 K*)   N(3) 264.8

Figure 2. Synthetically-relevant *N*-brominated species and their corresponding N—Br BDEs (obtained using the G3-B3 protocol).

Regarding the choice of reference wave function, we observe that the restricted procedures generally offer better performance than their unrestricted counterparts, a result that is consistent with previous findings for the calculation of C–H BDEs.[114] For the second-order methods (i.e., UMP2 vs ROMP2), a very large difference in the RMSD is noted (26.6 kJ mol^{-1}). For the forth-order methods, while only a residual difference (0.3 kJ mol^{-1}) is noted in the case of the (U/RO)MP4(SDQ) procedures, a larger difference (16.6 kJ mol^{-1}) is observed when comparing UMP4(SDTQ) and ROMP4(SDTQ). In terms of the third-order methods, although UMP3 and ROMP3 exhibit comparable RMSDs (which differ by just 0.1 kJ mol^{-1}), the LD for ROMP3 (17.2 kJ mol^{-1}) is substantially smaller than that for UMP3 (29.0 kJ mol^{-1}). Considering the LDs of the unrestricted procedures more generally, we see that for all such methods, molecule **13** ((NC)CONHBr) provides the most challenging test. This is perhaps not unexpected, given that the product radical, (NC)CONH$^•$, is associated with the largest degree of spin contamination of all of the considered radicals ($\langle s^2 \rangle = 1.08$). The use of a restricted open-shell formalism overcomes this difficulty with great effectiveness. For example, although the deviation for molecule **13** at the UMP2 level is 117.7 kJ mol^{-1}, the deviation at the ROMP2 level is reduced to 41.4 kJ mol^{-1}.

Regarding the performance of the spin-component-scaled Møller–Plesset procedures (SCS-MPn), we note that: (i) the SCS-ROMP2 procedure offers a negligible improvement over ROMP2 (by just 0.4 kJ mol^{-1}), and (ii) the SCS-ROMP3 procedure is substantially worse than ROMP3 (with an RMSD increase of 12.3 kJ mol^{-1}). As a result, we see no benefit in the use of SCS-MPn procedures for the calculation of N–Br BDEs.

Of particular interest is the finding that the recently defined ROMP4$_{av}$ (i.e., the average of the ROMP4(SDQ) and ROMP4(SDTQ) energies) and ROMP3.5 (i.e., the average of the ROMP3 and ROMP4(SDTQ) energies) procedures offer excellent performance (RMSDs = 5.7 and 5.4 kJ mol^{-1}, respectively), that even surpasses that of the considerably more costly URCCSD(T) method (RMSD = 6.0 kJ mol^{-1}). Furthermore, in contrast to URCCSD(T), which tends to underestimate the BDEs (MSD = −5.9 kJ mol^{-1}), the ROMP4$_{av}$ and ROMP3.5 procedures have a tendency to overestimate the BDEs (MSDs = +3.7 and +3.4 kJ mol^{-1}, respectively).

N—Br bond energies of selected synthetically-important molecules

Having identified that the G3-B3 thermochemical protocol offers excellent performance for the calculation of homolytic

N—Br BDEs (with an RMSD and LD of 2.9 and 5.2 kJ mol^{-1}, respectively, Table 4), we herein use this method for obtaining the BDEs (at 298 K) for four larger molecules that are widely used in synthetic organic chemistry and industry. The molecules chosen include (Fig. 2): N-bromosuccinimide (**19**), N-bromoglutarimide (**20**), N-bromophthalimide (**21**), and 1,3-dibromo-5,5-dimethylhydantoin (**22**).

Beginning with the BDE of the ubiquitous brominating agent N-bromosuccinimide (**19**), we compute a value of 281.6 kJ mol^{-1}, which is in reasonable agreement with the experimentally reported value of 276.1 ± 8.4 kJ mol^{-1}.[115] We wish to mention that the previously reported BDE of 265.2 kJ mol^{-1} (obtained at the B3LYP/6-311++G(d,p) level)[116] appears to be too low, and this is consistent with our findings that B3LYP significantly underestimates N—Br BDEs (Table 2). Increasing the ring size from five to six, as in N-bromoglutarimide (**20**) results in a significant decrease in the strength of the N—Br bond (by 18.4 kJ mol^{-1}). Our computed BDE of 263.2 kJ mol^{-1} for **20** is at the lower end of the experimentally reported value of 272.0 ± 8.4 kJ mol^{-1}.[115] In the light of this, a reevaluation of the experimental value of **20** seems in order.

The larger BDE of **19** vs. **20** arises because of two effects. First, the dissociation of **19** requires that stronger stabilizing lone-pair → $\pi^*_{C=O}$ interactions present in the closed-shell parent be disrupted upon formation of the product radicals (which both adopt π-ground states, in agreement with previous findings[97]), compared with the same interactions in **20**. In this regard, NBO calculations at the B3LYP/A′VTZ level indicate that each of the two stabilizing interactions ($E_{(2)}$) in **19** amount to 191.0 kJ mol^{-1} compared with 186.6 kJ mol^{-1} in the case of **20**. Second, as has been reported previously,[117] the succinimidyl radical has a greater proportion of the unpaired electron on the more electronegative oxygen atoms compared with glutarimidyl. It is also of interest to point out that the 18.4 kJ mol^{-1} decrease in N—Br BDEs observed upon going from **19** to **20** is of comparable magnitude to the difference in N—H BDEs (17.2 kJ mol^{-1}) between succinimide and glutarimide reported previously.[117]

The BDE of N-bromophthalimide (**21**, 274.7 kJ mol^{-1}) is computed to be slightly lower than that of **19** (281.6 kJ mol^{-1}). This may be attributed, in part, to the fact that the magnitude of stabilizing nitrogen lone-pair → $\pi^*_{C=O}$ interactions that must be overcome in dissociating **21** are smaller than in the case of **19** ($E_{(2)}$ = 187.3 vs. 191.0 kJ mol^{-1}, respectively). Electron spin resonance (ESR) studies have unambiguously confirmed that the phthalimidyl radical adopts a π-ground state.[118] Resonance effects in **21** between the two C=O groups and the aromatic ring system ($E_{(2)}$ = 76.5 kJ mol^{-1} per interaction), the likes of which are not present in **19**, likely contribute to the reduced stabilizing nitrogen lone-pair → $\pi^*_{C=O}$ interaction in the former. We additionally wish to note that point out that the π-ground state of the phthalimidyl radical has been confirmed on the basis of ESR studies.

Attention is now turned to the strengths of the two N—Br bonds in 1,3-dibromo-5,5-dimethylhydantoin (**22**). This compound is gaining widespread interest as a cheap and effective alternative to N-bromosuccinimide (**19**), and has wide ranging applications. Examples of its use in organic synthesis include: (i) the bromination of activated benzoic acids,[119] (ii) the solvent-free oxidation of secondary alcohols,[120] and (iii) the oxidation of isoxazolines,[121] thiols,[122] and benzylic alcohols.[123] It has also used as an analytical reagent for the determination of numerous analgesics[124,125] and antihistamines.[126] Regarding the strength of the N—Br bonds in **22**, for the $N_{(1)}$—Br bond, we compute a BDE of 218.2 kJ mol^{-1}, while for the $N_{(3)}$—Br bond, the BDE is found to be 264.8 kJ mol^{-1}. The weaker nature of the $N_{(1)}$—Br vs. $N_{(3)}$—Br bond may be accounted for, in part, on the basis that whereas dissociation of the $N_{(1)}$—Br bond requires significant disruption of only one stabilizing lone-pair → $\pi^*_{C=O}$ interaction on going from the closed-shell parent to the product radical ($E_{(2)}$ = 212.1 kJ mol^{-1}, based on NBO calculations at the B3LYP/A′VTZ level), two such interactions must be disrupted upon cleavage of the $N_{(3)}$—Br bond ($E_{(2)}$ = 165.1 and 225.7 kJ mol^{-1}).

Conclusions

We have obtained homolytic N—Br BDEs for a set of 18 molecules using the highly accurate W2 thermochemical protocol. As little is known about the strength of N—Br bonds toward homolytic cleavage, this set fills this apparent void. The BDEs (at 298 K) range from 162.2 kJ mol^{-1} for N-bromopyrrole to 260.6 kJ mol^{-1} for (CHO)$_2$NBr. Substituent effects have been analyzed on the basis of Mulliken spin densities, and NBO calculations. Using the all-electron, nonrelativistic, electronic W2 BDEs as reference values, we have assessed the performance of a wide range of contemporary DFT, DHDFT, composite and standard ab initio methods for the calculation of N—Br BDEs. With regard to the performance of these methods, we make the following general observations:

Of the 53 conventional DFTs, none attain RMSDs below the threshold of chemical accuracy ($\leq$ 4.2 kJ mol^{-1}). The best performing methods (with RMSDs in parentheses) are: BMK-D3 (7.0), MN12-SX (7.4), M11 (7.4), and M06-HF (7.8 kJ mol^{-1}). The worst performing method is BH&HLYP (55.4 kJ mol^{-1}), but the popular functional B3LYP also exhibits poor performance (31.1 kJ mol^{-1}).

Of the considered double-hybrid DFT procedures, PWPB95-D3 offers the best performance (RMSD = 4.3 kJ mol^{-1}), while B2-PLYP-D3 and B2GP-PLYP-D3 are the next best performing methods, both exhibiting RMSDs of 5.7 kJ mol^{-1}. Both of the latter procedures perform substantially better than their nondispersion-corrected parents, namely B2-PLYP and B2GP-PLYP, which have RMSDs of 10.6 and 7.7 kJ mol^{-1}, respectively. The worst DHDFT considered is DSD-PBEP86-D3, with an RMSD of 11.6 kJ mol^{-1}.

Regarding the performance of the composite thermochemical protocols, G3-B3 achieves excellent results, with an RMSD and LD of 2.9 and 5.2 kJ mol^{-1}, respectively. The reduced order variant G3(MP2)-B3 offers performance (RMSD = 4.2 kJ mol^{-1}) that is slightly worse than G3-B3, but which is comparable to the more costly G4 procedure (RMSD = 4.3 kJ mol^{-1}).

The CBS-QB3 procedure is the worst performing of the composite methods (RMSD = 9.8 kJ mol^{-1}), but the restricted-open-shell variant ROCBS-QB3 offers a significant improvement (RMSD = 4.5 kJ mol^{-1}).

Of the standard *ab initio* procedures that we have considered, we make the following conclusions: (i) The use of a spin-restricted wave function offers improved performance compared with using an unrestricted formalism, (ii) the UMP2 and ROMP2 procedures are inadequate for the calculation of N—Br BDEs (RMSDs = 60.7 and 34.1 kJ mol^{-1}, respectively), and (iii) the (U/RO)MP4(SDQ) procedures offer reasonable performance (RMSDs = 10.3 and 10.0 kJ mol^{-1}), but that the (U/RO)MP4(SDTQ) methods offer substantially worse performance (RMSDs = 33.8 and 17.2 kJ mol^{-1}).

We find that the recently defined ROMP4$_{av}$ and ROMP3.5 procedures offer excellent performance (RMSDs = 5.7 and 5.4 kJ mol^{-1}, respectively), that even surpasses that of the considerably more costly URCCSD(T) method (RMSD = 6.0 kJ mol^{-1}).

Finally, having ascertained the high reliability of the G3-B3 thermochemical protocol, we have applied this method toward the calculation of the N—Br BDEs of four species widely employed in synthetic and industrial chemistry. For the following molecules, we compute BDEs (at 298 K) of: *N*-bromosuccinimide (281.6), *N*-bromoglutarimide (263.2), *N*-bromophthalimide (274.7), and 1,3-dibromo-5,5-dimethylhydantoin (218.2 and 264.8 kJ mol^{-1}).

Acknowledgments

[1] P. Kovacic, M. K. Lowery, K. W. Field, *Chem. Rev.* **1970**, *70*, 639.
[2] I. V. Koval, *Russ. J. Org. Chem.* **2002**, *38*, 301.
[3] E. Kolvari, A. Ghorbani-Choghamarani, P. Salehi, F. Shirini, M. A. Zolfigol, *J. Iran. Chem. Soc.* **2007**, *4*, 126.
[4] D. I. Pattison, M. J. Davies, *Curr. Med. Chem.* **2006**, *13*, 3271.
[5] M. D. Rees, T. N. McNiven, M. J. Davies, *Biochem. J.* **2007**, *401*, 587.
[6] O. Skaff, D. I. Pattison, M. J. Davies, *Chem. Res. Toxicol.* **2007**, *20*, 1980.
[7] C. L. Hawkins, M. J. Davies, *Free Radic. Biol. Med.* **2005**, *39*, 900.
[8] G. Sun, L. C. Allen, E. P. Luckie, W. B. Wheatley, S. D. Worley, *Ind. Eng. Chem. Res.* **1995**, *34*, 4106.
[9] V. S. Panangala, L. Liu, G. Sun, S. D. Worley, A. Mitra, *J. Virol. Methods.* **1997**, *66*, 263.
[10] O. Aviv, S. Farah, N. Amir, N. Laout, S. Ratner, A. J. Domb, *Biomacromolecules.* **2015**, *16*, 1442.
[11] T. C. Tsao, D. E. Williams, C. G. Worley, S. D. Worley, *Biotechnol. Prog.* **1991**, *7*, 60.
[12] C. K. Tan, Y. –Y. Yeung, *Chem. Commun.* **2013**, *49*, 7985.
[13] E. J. Corey, W. R. Hertler, *J. Am. Chem. Soc.* **1960**, *82*, 1657.
[14] U. Wille, O. Krüger, A. Kirsch, U. Lüning, *Eur. J. Org. Chem.* **1999**, 3185.
[15] V. A. Schmidt, R. K. Quinn, A. T. Brusoe, E. J. Alexanian, *J. Am. Chem. Soc.* **2014**, *136*, 14389.
[16] C. G. McCarty, C. G. Leeper, *J. Org. Chem.* **1970**, *35*, 4245.
[17] J. M. L. Martin, G. Oliveira, *J. Chem. Phys.* **1999**, *111*, 1843.
[18] T. H. Dunning, Jr., *J. Chem. Phys.* **1989**, *90*, 1007.
[19] A. K. Wilson, D. E. Woon, K. A. Peterson, T. H. Dunning, Jr. *J. Chem. Phys.* **1999**, *110*, 7667.
[20] J. P. Merrick, D. Moran, L. Radom, *J. Phys. Chem. A* **2007**, *111*, 11683.
[21] Gaussian 09, Revision D.01, M. J. Frisch, G. W. Trucks, H. B. Schlegel, G. E. Scuseria, M. A. Robb, J. R. Cheeseman, G. Scalmani, V. Barone, B. Mennucci, G. A. Petersson, H. Nakatsuji, M. Caricato, X. Li, H. P. Hratchian, A. F. Izmaylov, J. Bloino, G. Zheng, J. L. Sonnenberg, M. Hada, M. Ehara, K. Toyota, R. Fukuda, J. Hasegawa, M. Ishida, T. Nakajima, Y. Honda, O. Kitao, H. Nakai, T. Vreven, J. A. Montgomery, Jr., J. E. Peralta, F. Ogliaro, M. Bearpark, J. J. Heyd, E. Brothers, K. N. Kudin, V. N. Staroverov, R. Kobayashi, J. Normand, K. Raghavachari, A. Rendell, J. C. Burant, S. S. Iyengar, J. Tomasi, M. Cossi, N. Rega, J. M. Millam, M. Klene, J. E. Knox, J. B. Cross, V. Bakken, C. Adamo, J. Jaramillo, R. Gomperts, R. E. Stratmann, O. Yazyev, A. J. Austin, R. Cammi, C. Pomelli, J. W. Ochterski, R. L. Martin, K. Morokuma, V. G. Zakrzewski, G. A. Voth, P. Salvador, J. J. Dannenberg, S. Dapprich, A. D. Daniels, ø. Farkas, J. B. Foresman, J. V. Ortiz, J. Cioslowski, and D. J. Fox, Gaussian, Inc., Wallingford CT, **2009**.
[22] H.-J. Werner, P. J. Knowles, G. Knizia, F. R. Manby, M. Schütz, P. Celani, T. Korona, R. Lindh, A. Mitrushenkov, G. Rauhut, K. R. Shamasundar, T. B. Adler, R. D. Amos, A. Bernhardsson, A. Berning, D. L. Cooper, M. J. O. Deegan, A. J. Dobbyn, F. Eckert, E. Goll, C. Hampel, A. Hesselmann, G. Hetzer, T. Hrenar, G. Jansen, C. Köppl, Y. Liu, A. W. Lloyd, R. A. Mata, A. J. May, S. J. McNicholas, W. Meyer, M. E. Mura, A. Nicklass, D. P. O'Neill, P. Palmieri, D. Peng, K. Pflüger, R. Pitzer, M. Reiher, T. Shiozaki, H. Stoll, A. J. Stone, R. Tarroni, T. Thorsteinsson, and M. Wang, Available at http:www.molpro.net.
[23] S. Parthiban, G. de Oliveira, J. M. L. Martin, *J. Phys. Chem. A* **2001**, *105*, 895.
[24] M. Douglas, N. M. Kroll, *Ann. Phys.* **1974**, *82*, 89.
[25] B. A. Hess, *Phys. Rev. A* **1986**, *33*, 3742.
[26] L. A. Curtiss, M. P. McGrath, J. P. Blaudeau, N. E. Davis, R. Binning, *J. Chem. Phys.* **1995**, *103*, 6104.
[27] J. P. Perdew, K. Schmidt, *AIP Conf. Proc.* **2001**, *577*, 1.
[28] C. Lee, W. Yang, R. G. Parr, *Phys. Rev. B* **1988**, *37*, 785.
[29] A. D. Becke, *Phys. Rev. A* **1988**, *38*, 3098.
[30] S. Grimme, *J. Comput. Chem.* **2006**, *27*, 1787.
[31] A. D. Boese, N. C. Handy, *J. Chem. Phys.* **2001**, *114*, 5497.
[32] (a) J. P. Perdew, K. Burke, M. Ernzerhof, *Phys. Rev. Lett.* **1996**, *77*, 3865; (b) J. P. Perdew, K. Burke, M. Ernzerhof, *Phys. Rev. Lett.* **1997**, *78*, 1396.
[33] J. P. Perdew, *Phys. Rev. B* **1986**, *33*, 8822.
[34] R. Peverati, Y. Zhao, D. G. Truhlar, *J. Phys. Chem. Lett.* **2011**, *2*, 1991.
[35] R. Peverati, D. G. Truhlar, *J. Chem. Theory Comput.* **2012**, *8*, 2310.
[36] Y. Zhao, D. G. Truhlar, *J. Chem. Phys.* **2006**, *125*, 194101.
[37] J. M. Tao, J. P. Perdew, V. N. Staroverov, G. E. Scuseria, *Phys. Rev. Lett.* **2003**, *91*, 146401.
[38] A. D. Boese, N. C. Handy, *J. Chem. Phys.* **2002**, *116*, 9559.
[39] T. van Voorhis, G. E. Scuseria, *J. Chem. Phys.* **1998**, *109*, 400.
[40] R. Peverati, D. G. Truhlar, *J. Phys. Chem. Lett.* **2012**, *3*, 117.
[41] R. Peverati, D. G. Truhlar, *Phys. Chem. Chem. Phys.* **2012**, *10*, 13171.
[42] A. D. Becke, *J. Chem. Phys.* **1993**, *98*, 1372.
[43] P. J. Stephens, F. J. Devlin, C. F. Chabalowski, M. J. Frisch, *J. Phys. Chem.* **1994**, *98*, 11623.
[44] A. D. Becke, *J. Chem. Phys.* **1993**, *98*, 5648.
[45] J. P. Perdew, J. A. Chevary, S. H. Vosko, K. A. Jackson, M. R. Pederson, D. J. Singh, C. Fiolhais, *Phys. Rev. B* **1992**, *46*, 6671.

[46] C. Adamo, V. Barone, *J. Chem. Phys.* **1999**, *110*, 6158.

[47] F. A. Hamprecht, A. J. Cohen, D. J. Tozer, N. C. Handy, *J. Chem. Phys.* **1998**, *109*, 6264.

[48] H. L. Schmider, A. D. Becke, *J. Chem. Phys.* **1998**, *108*, 9624.

[49] X. Xu, Q. Zhang, R. P. Muller, W. A. Goddard, *J. Chem. Phys.* **2005**, *122*,

[50] R. Peverati, D. G. Truhlar, *J. Chem. Phys.* **2011**, *135*, 191102.

[51] Y. Zhao, N. E. Schultz, D. G. Truhlar, *J. Chem. Phys.* **2005**, *123*, 161103.

[52] Y. Zhao, N. E. Schultz, D. G. Truhlar, *J. Chem. Theory Comput.* **2006**, *2*, 364.

[53] Y. Zhao, D. G. Truhlar, *Theor. Chem. Acc.* **2008**, *120*, 215.

[54] A. D. Boese, J. M. L. Martin, *J. Chem. Phys.* **2004**, *121*, 3405.

[55] A. D. Becke, *J. Chem. Phys.* **1996**, *104*, 1040.

[56] Y. Zhao, D. G. Truhlar, *J. Phys. Chem. A* **2005**, *109*, 5656.

[57] V. N. Staroverov, G. E. Scuseria, J. Tao, J. P. Perdew, *J. Chem. Phys.* **2003**, *119*, 12129.

[58] L. Goerigk, S. Grimme, *WIREs Comput. Mol. Sci.* **2014**, *4*, 576.

[59] S. Grimme, *J. Chem. Phys.* **2006**, *124*, 034108.

[60] D. C. Graham, A. S. Menon, L. Goerigk, S. Grimme, L. Radom, *J. Phys. Chem. A* **2009**, *113*, 9861.

[61] A. Karton, A. Tarnopolsky, J. –F. Lamere, G. C. Schatz, J. M. L. Martin, *J. Phys. Chem. A* **2008**, *112*, 12868.

[62] A. Tarnopolsky, A. Karton, R. Sertchook, D. Vuzman, J. M. L. Martin, *J. Phys. Chem. A* **2008**, *112*, 3.

[63] S. Kozuch, D. Gruzman, J. M. L. Martin, *J. Phys. Chem. C* **2010**, *114*, 20801.

[64] S. Kozuch, J. M. L. Martin, *Phys. Chem. Chem. Phys.* **2011**, *12*, 20104.

[65] S. Kozuch, J. M. L. Martin, *J. Comput. Chem.* **2013**, *34*, 2327.

[66] L. Goerigk, S. Grimme, *J. Chem. Theory Comput.* **2011**, *7*, 291.

[67] T. Yanai, D. Tew, N. Handy, *Chem. Phys. Lett.* **2004**, *393*, 51.

[68] O. A. Vydrov, G. E. Scuseria, *J. Chem. Phys.* **2006**, *125*, 34109.

[69] J. D. Chai, M. Head-Gordon, *J. Chem. Phys.* **2008**, *128*, 084106.

[70] J. D. Chai, M. Head-Gordon, *Phys. Chem. Chem. Phys.* **2008**, *10*, 6615.

[71] J. Heyd, G. E. Scuseria, M. Ernzerhof, *J. Chem. Phys.* **2003**, *118*, 8207.

[72] T. M. Henderson, A. F. Izmaylov, G. E. Scuseria, A. Savin, *J. Chem. Theory Comput.* **2008**, *4*, 1254.

[73] R. Peverati, D. G. Truhlar, *Phys. Chem. Chem. Phys.* **2012**, *14*, 16187.

[74] R. Peverati, D. G. Truhlar, *J. Phys. Chem. Lett.* **2011**, *2*, 2810.

[75] S. Grimme, E. Ehrlich, L. Goerigk, *J. Comput. Chem.* **2011**, *32*, 1456.

[76] S. Grimme, J. Antony, S. Ehrlich, H. Krieg, *J. Chem. Phys.* **2010**, *132*, 154104.

[77] S. Grimme, *WIREs Comput. Mol. Sci.* **2011**, *1*, 211.

[78] A. D. Becke, E. R. Johnson, *J. Chem. Phys.* **2005**, *13*, 154101.

[79] A. Karton, J. M. L. Martin, *J. Chem. Phys.* **2011**, *135*, 144119.

[80] L. A. Curtiss, P. C. Redfern, K. Raghavachari, *J. Chem. Phys.* **2007**, *126*, 084108.

[81] L. A. Curtiss, P. C. Redfern, K. Raghavachari, *J. Chem. Phys.* **2007**, *127*, 124105.

[82] B. Chan, J. Deng, L. Radom, *J. Chem. Theory Comput.* **2011**, *7*, 112.

[83] A. G. Baboul, L. A. Curtiss, P. C. Redfern, K. Raghavachari, *J. Chem. Phys.* **1999**, *110*, 7650.

[84] (a) J. A. Montgomery, Jr., M. J. Frisch, J. W. Ochterski, G. A. Petersson, *J. Chem. Phys.* **1999**, *110*, 2822; (b) J. A. Montgomery, Jr., M. J. Frisch, J. W. Ochterski, G. A. Petersson, **2000**, *112*, 6532.

[85] G. P. F. Wood, L. Radom, G. A. Petersson, E. C. Barnes, M. J. Frisch, J. A. Montgomery, Jr., *J. Chem. Phys.* **2006**, *125*, 094106.

[86] S. Grimme, *J. Chem. Phys.* **2003**, *118*, 9095.

[87] A. Karton, L. Goerigk, *J. Comput. Chem.* **2015**, *36*, 622.

[88] S. Grimme, *J. Comput. Chem.* **2003**, *24*, 1529.

[89] L. J. Yu, F. Sarrami, R. J. O'Reilly, A. Karton, *Chem. Phys.* **2015**, *458*, 1.

[90] U. Becker, D. Bykov, D. Ganyushin, A. Hansen, R. Izsak, D. G. Liakos, C. Kollmar, S. Kossmann, D. A. Pantazis, T. Petrenko, C. Reimann, C. Riplinger, M. Roemelt, B. Sandhöfer, I. Schapiro, K. Sivalingam, F. Wennmohs, B. Wezisla and contributions from our collaborators: M. Kállay, S. Grimme, E. Valeev. Mülheim: Max Planck Institute for Chemical Energy Conversion, **2014**.

[91] F. Neese, *WIREs Comput. Mol. Sci.* **2012**, *2*, 73.

[92] J. P. Foster, F. Weinhold, *J. Am. Chem. Soc.* **1980**, *102*, 7211.

[93] A. Karton, E. Rabinovich, J. M. L. Martin, B. Ruscic, *J. Chem. Phys.* **2006**, *125*, 144108.

[94] A. Karton, J. M. L. Martin, *J. Chem. Phys.* **2010**, *133*, 144102.

[95] A. Karton, S. Daon, J. M. L. Martin, *Chem. Phys. Lett.* **2011**, *510*, 165.

[96] H. Zipse, *Top. Curr. Chem.* **2006**, *263*, 163.

[97] J. Hioe, D. Sakic, V. Vrcek, H. Zipse, *Org. Biomol. Chem.* **2015**, *13*, 157.

[98] G. P. F. Wood, D. J. Henry, L. Radom, *J. Phys. Chem. A* **2003**, *107*, 7985.

[99] Y. Apeloig, R. Schreiber, *J. Am. Chem. Soc.* **1980**, *102*, 6144.

[100] H. M. Muchall, N. H. Werstiuk, J. Lessard, *J. Mol. Struct. (THEOCHEM)* **1999**, *469*, 135.

[101] J. Lessard, D. Griller, K. U. Ingold, *J. Am. Chem. Soc.* **1980**, *102*, 3262.

[102] R. Sutcliffe, D. Griller, J. Lessard, K. U. Ingold, *J. Am. Chem. Soc.* **1981**, *103*, 624.

[103] H. Teeninga, J. B. F. N. Engberts, *Tetrahedron Lett.* **1982**, *23*, 1007.

[104] W. C. Danen, R. W. Gellert, *J. Am. Chem. Soc.* **1972**, *94*, 6853.

[105] E. P. Oliveto, C. Gerold, *Org. Synth.* **1951**, *31*, 17.

[106] D. Colbourne, D. C. Frost, C. A. McDowell, N. P. C. Westwood, *Can. J. Chem.* **1979**, *57*, 1279.

[107] F. Carnovale, E. Nagy-Felsobuki, J. B. Peel, G. D. Willett, *J. Electron. Spectrosc. Relat. Phenom.* **1978**, *14*, 163.

[108] M. Funatsu, N. M. Green, B. Witkop, *J. Am. Chem. Soc.* **1964**, *86*, 1846.

[109] W. H. Liu, T. Beppu, K. Arima, *Agric. Biol. Chem.* **1977**, *41*, 131.

[110] M. D. Rosa, *J. Org. Chem.* **1982**, *47*, 1008.

[111] R. J. O'Reilly, A. Karton, L. Radom, *J. Phys. Chem. A* **2011**, *115*, 5496.

[112] G. A. Cordell, *J. Org. Chem.* **1975**, *40*, 3161.

[113] R. J. O'Reilly, A. Karton, L. Radom, *Int. J. Quantum Chem.* **2012**, *112*, 1862.

[114] C. J. Parkinson, P. M. Mayer, L. Radom, *J. Chem. Soc., Perkin Trans. 2* **1999**, *11*, 2305.

[115] Y.-R. Luo, Comprehensive Handbook of Chemical Bond Energies; Taylor & Francis: Boca Raton, FL, **2007** (and references therein).

[116] S. A. K. Elroby, M. A. Noamaan, M. F. Shibl, *J. Mol. Struct. (THEOCHEM)* **2009**, *915*, 93.

[117] R. J. O'Reilly, A. Karton, L. Radom, *J. Phys. Chem. A* **2013**, *117*, 460.

[118] P. H. Kasai, *J. Am. Chem. Soc.* **1992**, *114*, 2875.

[119] J. Auerbach, S. A. Weissman, T. J. Blacklock, M. R. Angeles, K. Hoogsteen, *Tetrahedron Lett.* **1993**, *34*, 931.

[120] A. Khazaei, F. Abbasi, M. Kianiborazjani, S. Saednia, *J. Braz. Chem. Soc.* **2014**, *25*, 361.

[121] D. Azarifar, B. Maleki, K. Mohammadi, *Heterocycles*, **2007**, *71*, 683.

[122] A. Khazaei, M. A. Zolfigol, A. Rostami, *Synthesis* **2004**, 2959.

[123] R. Liu, C. Dong, X. Liang, X. Wang, X. Hu, *J. Org. Chem.* **2005**, *70*, 729.

[124] K. Girish Kumar, R. Letha, *J. Pharm. Biomed. Anal.* **1997**, *15*, 1725.

[125] M. I. Walash, M. Rizk, F. Belal, A. Abo-Ouf, *Pharmazie*, **1979**, *34*, 234.

[126] K. Girish Kumar, L. Karpagaselvi, *Analyst*, **1994**, *119*, 1375.